NATIONAL AERONAUTICS AND SPACE ADMINISTRATION

MSC INTERNAL NOTE NO. 69-FM-163

June 16, 1969

AUTONOMOUS NAVIGATION IN LONG-DURATION HIGHLY ECCENTRIC ORBITS ABOUT MARS

Advanced Mission Design Branch

MISSION PLANNING AND ANALYSIS DIVISION

MANNED SPACECRAFT CENTER

HOUSTON, TEXAS

MSC INTERNAL NOTE NO. 69-FM-163

AUTONOMOUS NAVIGATION IN LONG-DURATION HIGHLY ECCENTRIC ORBITS ABOUT MARS

By Flora B. Lowes
Advanced Mission Design Branch

June 16, 1969

MISSION PLANNING AND ANALYSIS DIVISION
NATIONAL AERONAUTICS AND SPACE ADMINISTRATION
MANNED SPACECRAFT CENTER
HOUSTON, TEXAS

Approved: Jack Funk
Jack Funk, Chief
Advanced Mission Design Branch

Approved: for Carl R. Huss
John P. Mayer, Chief
Mission Planning and Analysis Division

CONTENTS

FIGURES

AUTONOMOUS NAVIGATION IN LONG-DURATION HIGHLY ECCENTRIC ORBITS ABOUT MARS

By Flora B. Lowes

1.0 SUMMARY

The problem of effective autonomous navigation for a manned spacecraft in highly eccentric orbits for long durations is considered. A statistical error analysis based on star-horizon, unknown landmark, and surface beacon measurements is presented for a 300-day orbital stay time about Mars. The data are processed with a Kalman filter, and the methods are evaluated for their applicability and effectiveness in the minimization of estimated state errors and in the production of reasonable measurement schedules. Results of the study indicate that the two optical angle measurement methods, although constrained by the orbital geometry, can be optimally combined and used for only 4 hours per day to produce an accuracy of less than 1 n. mi. The estimated error in the spacecraft position obtained by continuous onboard radar tracking of surface beacons is larger than that obtained with the optical navigation techniques. However, the result is highly dependent on the beacon location errors and was found to improve as the knowledge of the locations was increased.

2.0 INTRODUCTION

Future manned interplanetary missions, which will probably include lengthy planetary stopovers, place considerable emphasis on the study of the navigation problem of a manned spacecraft in highly eccentric, long-duration orbits. With future mission planning in mind and in anticipation of more dependence on autonomous navigation in interplanetary travel, it is important to evaluate state-of-the-art navigation techniques to determine those which are most effective and adaptive to such missions. Orbits with high eccentricities and which must be maintained over a long span of time offer a new opportunity for navigation study because limited information is available in this field; that is, most documented orbital navigation analyses have been performed for relatively short-duration and near-circular orbits.

A statistical error analysis is presented that is based on three types of orbital navigation techniques, star-horizon, unknown landmarks, and surface beacon tracking. The basic mathematical models of these navigation techniques can be found in the referenced literature. All methods are evaluated under the assumption that the data are processed with a Kalman filter. In the mathematical model, only sensor noise is considered for the unknown landmark navigation; however, for the other measurements, a dynamical bias is also included.

The study is initiated with orbital insertion at Mars periapsis and is terminated at transearth injection after a 300-day stay time. The initial position and velocity of the spacecraft are computed from a matched-conic interplanetary program (ref. 1) coupled with a navigation and guidance analysis program (ref. 2). An Earth-injection error matrix was propagated and updated during the trans-Mars phase of the mission by use of a combination of onboard optical and Earth-based radar tracking. Four midcourse guidance maneuvers were implemented and the error matrices were degraded each time because of assumed correction errors. The resultant navigation error matrix $E(t)$ after orbital deboost is used initially in this study to present a continuous analysis with realistic errors.

The purpose of the study is to determine the applicability of known autonomous navigation techniques for spacecraft in highly eccentric, long-duration orbits. The analysis is based on their capability to produce acceptable measurement schedules while enough information is produced to minimize estimated state errors.

The first section of the paper briefly reviews the reference mission chosen for the study. This section is followed by a description of the navigation system which involves the three navigational measurement types evaluated. Finally, the analysis data are presented in two parts in the results and discussion section: (1) data for the optical angle measurements (i.e., star-horizon and unknown landmarks), and (2) data for onboard beacon tracking.

3.0 SYMBOLS

c	designates body center in figure 2
E, E(t)	covariance matrix of state vector uncertainty
H, H(t)	sensitivity matrix
I	identity matrix

K	weighting matrix
M	matrix defined by equation (6)
Q	the measurable, as defined in equation (1)
R	covariance matrix of measurement errors
$\bar{r}$	position vector
r	position vector magnitude
r_p	planet radius
S(t)	transformation matrix that relates orbital element perturbations to perturbations in the Cartesian elements of position and velocity
$\bar{s}$	state vector (position and velocity)
SC	spacecraft
t	time
$\bar{u}(\ )$	unit vector in the direction of ( )
$\bar{V}$	velocity vector
α	angle defined in figure 2(a)
β	star-planet included angle (sextant)
θ	angle defined in figure 2(b)
ρ	range
$\dot{\rho}$	range rate
ρ_0	range at first sighting (unknown landmark)
ρ_1	range at second sighting (unknown landmark)
$\phi(t,t_0)$	state transition matrix evaluated between t and t_0

Subscripts:

s	star
vh	vehicle-planet horizon
vp	vehicle-planet center
ℓ	landmark

Superscripts:

T	transpose
-1	inverse
+	value after measurement
-	value before measurement

Operators:

$\nabla_{\bar{s}}(\ )$	gradient with respect to $\bar{s}$

4.0 ANALYSIS

4.1 Reference Mission

The representative orbit chosen for this study is taken from a 1977 Earth-Mars conjunction-class mission that involves a stay time of 300 days about the planet Mars. This orbit, the characteristics of which are given in table I, is highly eccentric with a periapsis altitude of 200 n. mi. and an apoapsis altitude of approximately 10 000 n. mi. This particular orbit was chosen as representative because of the opportunities it offers for overall mission planning in the areas of maximum scientific return and minimum fuel requirements (ref. 3), as well as for the versatility it permits in the application of navigational techniques. A schematic of the geometry of this Earth to Mars conjunction-class mission and the orbital period about Mars is shown in figure 1. This figure is taken from reference 4 in which detailed discussion of the orbit is contained.

4.2 Navigation System Description

Because the development of the pertinent navigation system equations and the descriptions of the navigational methods which pertain to them are thoroughly discussed in references 5 through 9, the following is only a brief summary of the principal equations used in this analysis.

The recursive navigation theory is used in which measurements are made along the trajectory and, in turn, are processed by a Kalman filter to improve the estimate of the state vector. For each measurement, a sensitivity matrix $H(t)$ is computed which relates measurement deviations to state vector deviations. This H matrix, expressed by

$$H(t) = \nabla_{\underline{s}} Q \tag{1}$$

where Q is the measurable, is associated with each type of navigation measurement made. As a result of each measurement and, thus, the calculation of the matrix $H(t)$, the covariance matrix $E(t)$ of state vector uncertainties is updated and then is propagated along the trajectory by the equation

$$E(t) = \phi(t,t_0)\, E(t_0)\, \phi^T(t,t_0) \tag{2}$$

where $\phi(t,t_0)$ is the state transition matrix evaluated between t_0 and t.

To avoid numerical difficulties in the update of the covariance matrix E, the standard form of the filter update equations given by

$$E^+ = (I - KH)E^- \tag{3}$$

can be written in the form

$$E^+ = (I - KH)\, E^-(I - KH)^T + KRK^T \tag{4}$$

where

$$K = EH^T M^{-1} \tag{5}$$

and

$$M = HEH^T + R \tag{6}$$

The matrix R in equation (6) is the covariance matrix of the errors in making the particular measurement.

For the three navigation observation types used in this study, the sensitivity matrix H can be written as follows.

1. For the star-horizon included-angle measurement, H is expressed as a 6 by 1 matrix defined by

$$H^T = \left[\begin{array}{c|c} \dfrac{\bar{u}_s - (\bar{u}_s \cdot \bar{u}_{vp})\bar{u}_{vp}}{r_{vp}\, r_{vh} \sin \beta} & 0 \end{array} \right] \tag{7}$$

where $\bar{u}_s$ and $\bar{u}_{vp}$ are the unit vectors from the spacecraft to the star and to the planet, respectively. The magnitudes r_{vp} and r_{vh} and the angle β are defined in figure 2(a) which shows the geometry of the star-horizon measurement.

2. For the unknown landmark navigation measurement, H is again expressed as a 6 by 1 matrix (ref. 5) defined by

$$H^T = \left[0 \;\middle|\; \bar{u}_{\rho_0} \times \bar{u}_{\rho_1} \right] \tag{8}$$

where $\bar{u}_{\rho_0}$ and $\bar{u}_{\rho_1}$ are the unit vectors from the spacecraft to the landmark at the first and second measurement times, respectively. The geometry of this measurement is shown in figure 2(b).

3. For the surface beacon measurement, the measurables are range ρ and range rate $\dot{\rho}$ of the spacecraft with respect to the beacon. Thus, the matrix H is of 6 by 2 dimension and is expressed by

$$H^T = \left[\begin{array}{c|c} \dfrac{\bar{u}_\rho}{(I - \bar{u}_\rho\, \bar{u}_\rho{}^T)\, \dfrac{\bar{V}_{slm}}{/\rho/}} & \begin{array}{c} 0 \\ \hline \bar{u}_\rho \end{array} \end{array} \right] \tag{9}$$

where $\bar{u}_\rho$ is the unit vector for the slant range measured from the spacecraft to the beacon, $\bar{V}_{slm}$ is the velocity vector of the spacecraft with respect to the beacon, and $/\rho/$ is the range magnitude. If either of the two measurements, range or range rate, is measured separately, the matrix in equation (9) would reduce to the 6 by 1 dimension composed of the respective row which pertained to the measurement processed.

These matrices can be augmented (ref. 9) to include the errors with respect to components other than position and velocity when needed (e.g., the inclusion of the estimation of beacon location errors).

The RMS (root-mean-square) position and velocity errors are computed directly from the covariance matrix of navigation errors $E(t)$. However, to present errors in the orbital element estimation, a transformation is involved. This operation is defined by

$$E'(t) = S(t)\, E(t)\, S^{T}(t) \tag{10}$$

where S is the transformation matrix that relates perturbations in the orbital elements to perturbations in the Cartesian components of position and velocity.

The assumed errors used for the navigation system are presented in table II.

5.0 RESULTS AND DISCUSSION

5.1 Optical Angle Measurements

The choice of the two optical measurements, star-horizon and unknown landmarks, for evaluation in this study was based on the assumption that either method could easily be applied to the mission considered. Both methods are relatively well known and easily implemented because all that are needed are an optical device such as the sextant, the planet, a catalogue of stars, and a man to make the measurements. Thus, for a manned mission which orbits about Mars, the application of these two navigation methods is dependent upon the restrictions imposed by the orbit itself. Some of the difficulties imposed by the highly eccentric orbit are the flatness of the trajectory and the extremities of the distances from the planet (i.e., very close at periapsis and far away at apoapsis). This particular orbit also offers other restrictions caused by its period of approximately 12 hours and by the surface lighting conditions. The orbit maintains its periapsis position in sunlight at all times; thus, only within approximately $\pm 90^{\circ}$ of periapsis is the surface in sunlight.

The star-horizon included-angle measurement is not restricted by surface lighting conditions. As long as the rim of the planet is visible and a recognizable star can be distinguished from the spacecraft, this particular measurement can be used. For the measurements in this study, the stars are chosen randomly from a computer star catalogue, and the planet rim used at all times is that of Mars.

It was found that the star-horizon measurement was used most effectively during the outer sections of the orbit, that is, not in the proximity of periapsis, because of the relatively short time phase of the orbit near periapsis and because of the low periapsis altitude which causes a number of the stars in the star catalogue to be occulted by Mars. Conversely, the outer portions of the orbit offer a free field for this measurement because of the distance and the majority of the orbital time spent there. The geometry of this measurement in figure 2(a) and the orbital characteristics in table I will provide a better understanding of the restrictions, measurements, and resultant data.

The RMS position uncertainty is plotted against the total time in orbit in figure 3(a). For this plot, star-horizon measurements only were made at 1-hour intervals for the entire orbital stay time. Although this schedule is unrealistic for man for 300 days, the figure is presented to establish a familiarity for this measurement and the level to which it reduces the estimated position uncertainties. Because of the magnitude of the time scale, the plot produced represents an error envelope in which only the upper and lower boundaries are distinguishable. However, the mean error produced is approximately 2.0 n. mi. To reduce the position uncertainties and keep them at a low level, the star-horizon measurement must be made often throughout the orbit.

As previously mentioned, the only part of the Martian surface which is lighted is that part within a 90° proximity of the periapsis line. Thus, when the unknown landmark navigation is considered, the measurements must be limited to a period of approximately 2 hours in the orbit when the spacecraft is near periapsis so that the surface features can be distinguished. The RMS position uncertainties are presented in figure 3(b) as a function of the total orbital time for unknown landmark measurements only. These measurements were used during each orbit while surface landmarks were visible. One set of measurements was made every 10 to 15 minutes. This measurement type is quite effective in the reduction of position uncertainties and results in an approximate mean error of 1 n. mi. [fig. 3(b)].

When the data obtained with the two optical measurements was evaluated, it was found that a combination of the two techniques is more effective in the reduction of measurement errors than is either technique when used individually. Each of the two techniques tends to compensate for the other's weaknesses caused by the high eccentricity of the orbit and the surface lighting conditions. Plotted data produced by the combination of these two measurement types are presented in figure 3(c). For this plot of RMS position uncertainties, star-horizon measurements were made at 15-minute intervals during the phase of the orbit between 160° and 195° true anomaly, and unknown landmark measurements were made at 15-minute intervals between 270° and 90° true anomaly. A further

restriction was that measurements were made only during every other orbit. Use of the combination of the two measurement types for approximately 4 hours of navigation per day (i.e., 2 hr in the vicinity of apoapsis and 2 hr in the vicinity of periapsis) is sufficient to maintain an accuracy of approximately 0.5 n. mi. for the orbital stay time [fig. 3(c)]. The combination of measurements not only produces acceptable accuracies but also provides a reasonable working schedule for the crewman by lowering the workload required for navigation measurements.

The RMS uncertainties in the orbital elements are presented in figure 4 for the previously discussed combined measurement schedule. These errors are plotted for the first 10 to 12 days only. However, this time length seems to be sufficient to analyze the effects in the orbital elements because as is evident from inspection of total position uncertainty plots, when the errors are reduced sufficiently, they are decreased very little during the rest of the orbital stay time. Instead, the errors are maintained at this decreased level by the optimal scheduling of the navigation measurements. Thus, the trends of the curves are already established by 10 days (fig. 4). The RMS uncertainty in the semimajor axis is presented in figure 4(a). From the plot, it can be seen that the error is rather large at the beginning of the mission but is decreased significantly to a very small uncertainty after 6 days of navigation measurements. The orbital element uncertainty curves for eccentricity and inclination are plotted in figures 4(b) and 4(c), respectively. The uncertainties of the three remaining orbital elements (true anomaly, ascending node, and argument of periapsis) are presented as three respective curves in figure 4(d). As expected, these curves follow the same trend as that for total position error and semimajor axis error, although they represent smaller values. Of all the elements, the uncertainty values for inclination appear to be most affected by the geometry of the orbit because it is the most oscillatory. However, the boundaries of the oscillation are reduced to values of near insignificance.

5.2 Onboard Beacon Tracking

Unmanned soft-landing probes (ref. 10) may be deployed from the orbiting manned spacecraft to study the Martian atmosphere and collect other scientific data. These probes could carry a transponder (called a beacon) for radar tracking by the orbiting spacecraft. In fact, this transponder capability may become the primary purpose of the probes. The beacons could provide almost continuous automatic tracking capability and would not be hampered by surface lighting conditions. Thus, in the study of beacon tracking, questions arise about the number of transponders needed on the surface, about where and when they should be deployed, and about how well their locations must be known for efficient orbital navigation about Mars.

The deployment of some of the beacons from the spacecraft may be accomplished during the trans-Mars portion of the mission. This deployment would depend upon the fuel budget allowed for the beacons. Targeting the beacons for either the northern or southern hemisphere would cost approximately the same if the beacons were deployed far enough away from Mars (ref. 10). Some of the beacons would be saved for deployment until the spacecraft had been in orbit for a period of time. However, this aspect involves a thorough, separate study and cannot be discussed in depth in this paper.

The study of onboard beacon tracking was initiated with 10 beacons placed at longitudes 36° apart. Because the orbital plane is in the northern part of the planet for approximately 10 hours of the total 12-hour orbital period, six of the beacons were placed in the northern hemisphere, and four were placed in the southern hemisphere. Later, the number of beacons was decreased to four, two in each hemisphere and spaced approximately 90° apart. When the beacons are spaced on the surface for continuous tracking capability, it must be remembered that two orbits are required before all of the planet is in view of the spacecraft because of the near 12-hour period of the orbit and the 24-hour rotational period of Mars. Line-of-sight radar visibility is assumed in the simulation regardless of the distance from the spacecraft to the surface beacon, except when the beacon is below the horizon.

A comparative study of range rate only and range/range-rate tracking by use of the beacons was made with sensor noise and beacon location errors included. For the conditions used, the addition of the range measurements to the range-rate tracking was found to contribute little significant data toward a decrease in the error values computed. Therefore, the presented data and discussion are for range-rate tracking only.

The RMS position uncertainty of the spacecraft is plotted as a function of time in figure 5 for range-rate tracking when 10 surface beacons are used. Measurements were made at 15-minute intervals, and no location errors were assumed in the beacon locations. As shown in the figure, the spacecraft position error is reduced quickly and remains close to the 0.25-n. mi. value. Although the data are plotted for only 11 days, the curve would be expected to continue at this low error value. This uncertainty curve is optimistic because it results from an assumption of no location errors assigned to the beacons.

To determine the effect of beacon location errors on the estimation of the state of the spacecraft, a 4-mile error in the longitude and latitude and a 6000-foot error in the altitude of the beacons' locations were assumed. The errors in the latitude and longitude were treated both deterministically as a bias and as a nondeterministic error source to be solved for in the filter. The altitude error was treated as a deterministic error only.

The RMS position uncertainty data are presented in figure 6 for range-rate measurements in 15-minute intervals, with 10 surface beacons, and with the previously mentioned location errors. This uncertainty curve represents the case in which the beacon latitude and longitude errors are estimated by use of the filter. The estimated spacecraft position uncertainty is oscillatory with the orbital period and, after 1 day of tracking, lies between the bounds of approximately 1.5 to 8 n. mi. (fig. 6). The figure is presented with the broken time scale so that the error obtained during the first 10 days of the orbital stay time can be compared to the error obtained 100 days later. As previously mentioned, when the error is reduced, it tends to continue at the reduced level with continued tracking.

Intuitively, the estimated beacon location errors might be expected to continue to decrease and, in turn, to reduce the spacecraft position uncertainty throughout the tracking period. However, this assumption is not true with the errors assumed because the estimated beacon location errors behave in the same manner as the estimated spacecraft state vector uncertainties; that is, they are reduced during the first few orbits to some level at which they tend to remain. In this case, it was found that the latitude error was reduced to approximately 0.25 n. mi., but the longitude error was reduced only to approximately 1.5 n. mi.; thus, sizable errors in the surface beacon locations were maintained.

The plotted data for the study in which the location errors are treated deterministically (i.e., the beacon location errors are not estimated) are not presented because they produced the same effects as seen in figure 6 with the exception that the error envelope was raised approximately 0.75 n. mi.

When the curve in figure 6 is compared to that in figure 5, it is evident that errors in the locations of surface beacons effectively raise the limits of the RMS position error curves. When the individual components of position error (i.e., altitude, range, and track) were examined, it was found that the altitude uncertainty is reduced very early to a small error value even when the beacons are assumed to have large location errors. The track uncertainty tends to decrease slowly and the down-range error, which maps into a timing error, remains the largest component of the total estimated position uncertainty.

The possibility was investigated that the amount of tracking might be increased during the early portions of the orbital mission so that the estimated errors in the beacon locations might be reduced and, thus, the spacecraft position uncertainty might be reduced. However, this increase in tracking was found to have little effect.

A simultaneous study with only four surface beacons was performed. The RMS position uncertainty of the spacecraft is plotted in figure 7 as a function of time in orbit for the same conditions and in the same manner as that in figure 6 except for the tracking of only four beacons. The use of the four beacons rather than 10 raises the upper bound of the estimated position error envelope approximately 4 n. mi. and the lower bound approximately 0.5 n. mi. In further study, it was found that if the locations of these four beacons were assumed to be better known the bounds of the error curve fell within the limits of that for the 10 beacons (fig. 6). Thus, the data tend to indicate that fewer beacons could be used if the ability to determine their locations is improved. A minimum of at least four surface beacons properly spaced for use in all orbits could provide enough information to the spacecraft for orbit maintenance based again on the knowledge of the locations of the beacons.

The uncertainties in the spacecraft orbital elements determined by use of surface beacon tracking are not plotted. The only element that showed any detectable error was the semimajor axis which maintained an oscillatory uncertainty between approximately 100 feet and 450 feet. The errors in the estimations of the other five orbital elements were reduced immediately to an insignificant level.

6.0 CONCLUDING REMARKS

For future mission planning, it is important to determine the effectiveness of some of the known autonomous navigation methods, as well as their adaptability to such missions. A statistical error analysis based on the use of star-horizon included-angle measurements, unknown landmarks, and surface beacons has been presented for navigation in a highly eccentric, long-duration orbit about Mars. It was found that these methods could be directly applied to such an orbit with only slight modification, but that the geometrical orbital restrictions must be considered in the optimal scheduling of navigation measurements.

The onboard optical measurements (unknown landmark and star-horizon) when used as a combination for 4 hours per day were found to produce an accuracy of less than 1 n. mi. for the 300-day orbital stay. It was also found that the use of these measurements in an optimal manner for the reduction of the crewman workload did not decrease this level of accuracy.

In contrast, the use of the surface beacons for radar tracking from the spacecraft does not reduce the estimated state errors as well as the optical measurements if fairly large beacon location errors are assumed. However, the beacon tracking does offer the advantage of almost continuous automatic tracking and is not hampered by lighting restrictions. Thus, for this type measurement to be of value, as compared to the optical measurements, an accurate technique to determine the beacon locations on the surface is required.

TABLE I.- CHARACTERISTICS OF MARS STOPOVER ORBIT

(1977 MARS MISSION)

Orbit stay time, days	300
Periapsis altitude, n. mi.	200
Apoapsis altitude, n. mi.	9621.67
Inclination, deg	18.65
Eccentricity	.697
Period, hr	11.78
Periapsis velocity in (hyperbola), fps	17 800
Periapsis velocity (ellipse), fps	14 403
Apoapsis velocity (ellipse), fps	2568
Periapsis velocity out (hyperbola), fps	18 395

TABLE II.- NOMINAL ROOT-MEAN-SQUARE ERROR VALUES IN NAVIGATION SYSTEM, 1σ

State position uncertainty, n. mi.	15
State velocity uncertainty, fps	61
Onboard sextant accuracy, arc sec	10
Optical error for unknown landmark sightings, arc min	1
Onboard radar accuracy	
Range	
Noise, ft	150
Bias, ft	15
Range rate	
Noise, fps	.6
Bias, fps	.03
Radius uncertainty/planet radius	.005

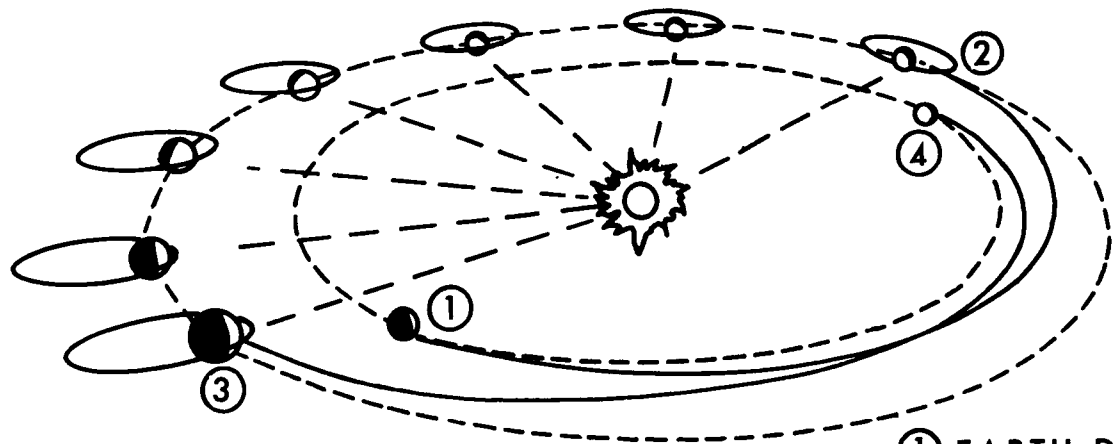

① EARTH DEPARTURE
② MARS ARRIVAL
③ MARS DEPARTURE
④ EARTH ARRIVAL

FIGURE 1.- HELIOCENTRIC SCHEMATIC ILLUSTRATING THE CONJUNCTION CLASS MISSION AND THE PARKING ORBIT ABOUT MARS.

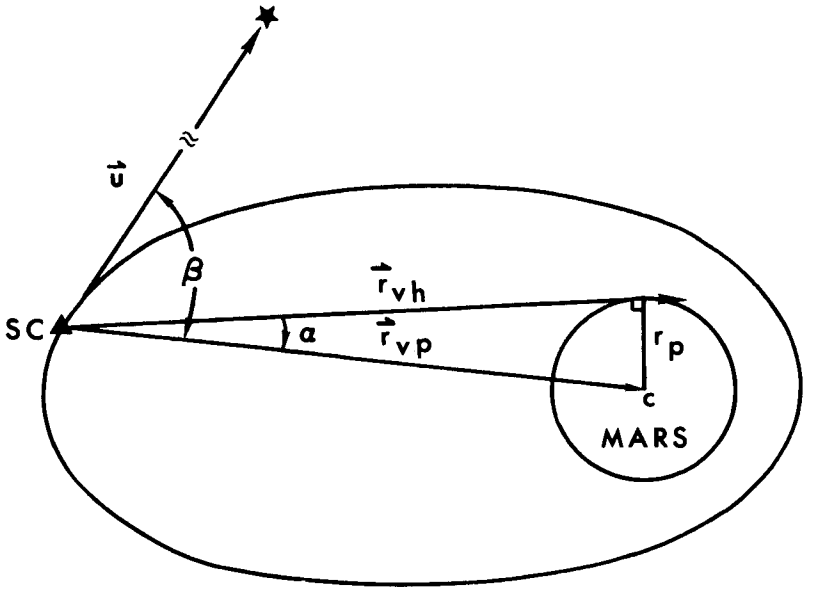

(A) GEOMETRY OF STAR-PLANET HORIZON INCLUDED-ANGLE MEASUREMENT.

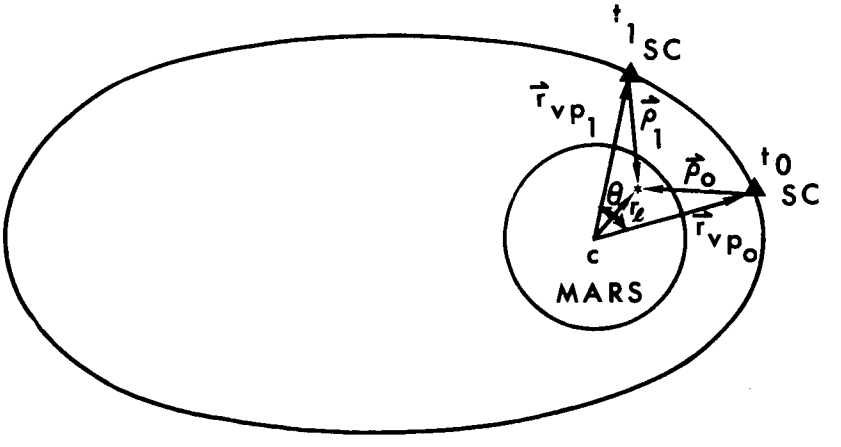

(B) GEOMETRY OF UNKNOWN-LANDMARK MEASUREMENT.

FIGURE 2.- GEOMETRY OF OPTICAL MEASUREMENTS USED IN ORBITAL NAVIGATION.

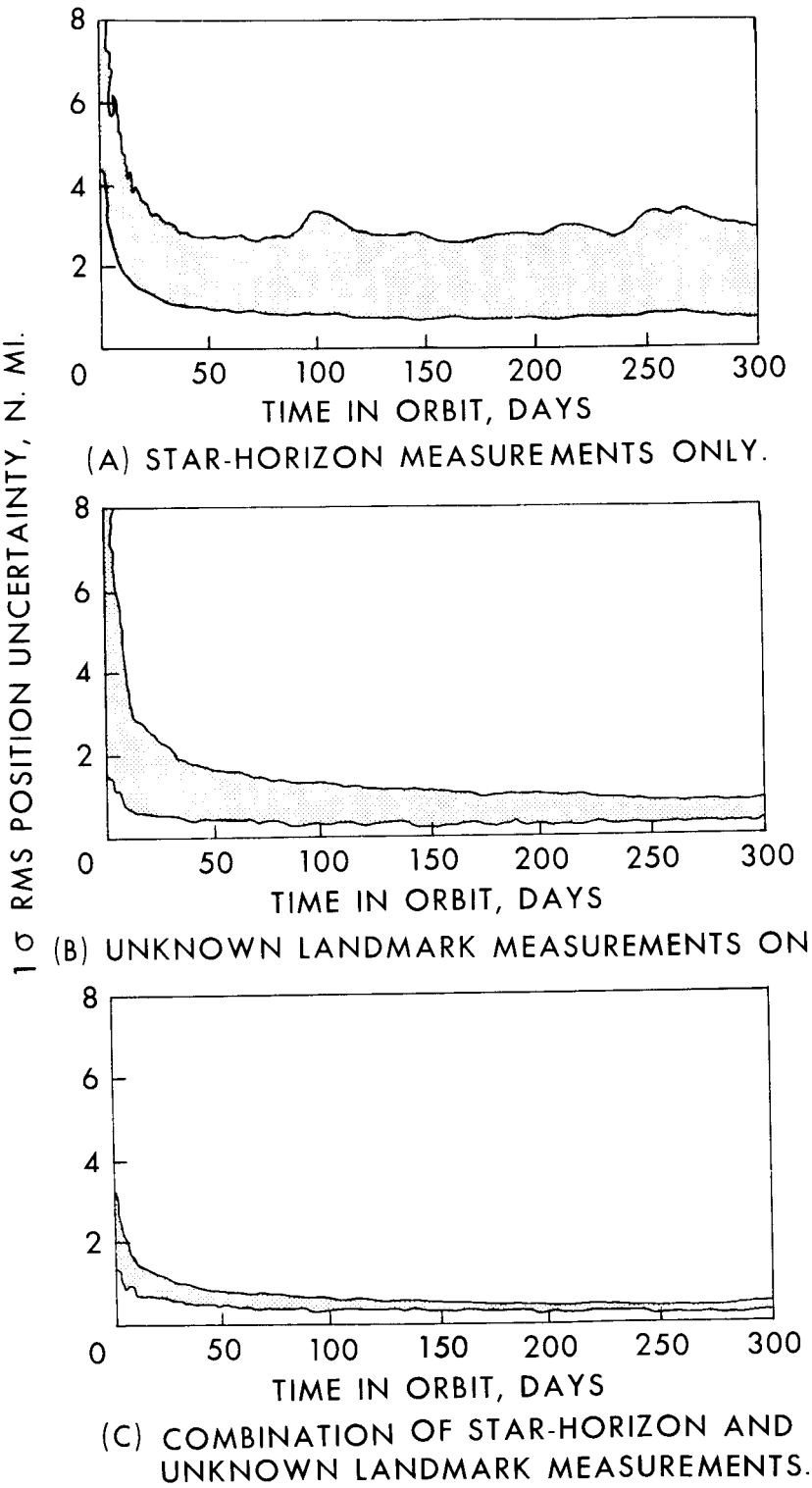

FIGURE 3.- RMS POSITION UNCERTAINTIES FOR OPTICAL NAVIGATION METHODS.

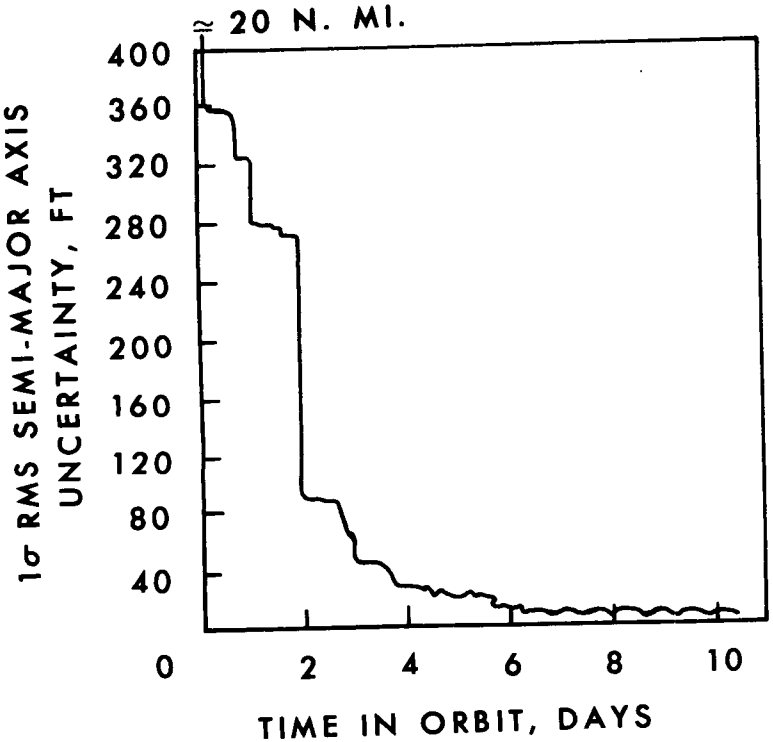

(A) RMS UNCERTAINTY FOR SEMI-MAJOR AXIS.

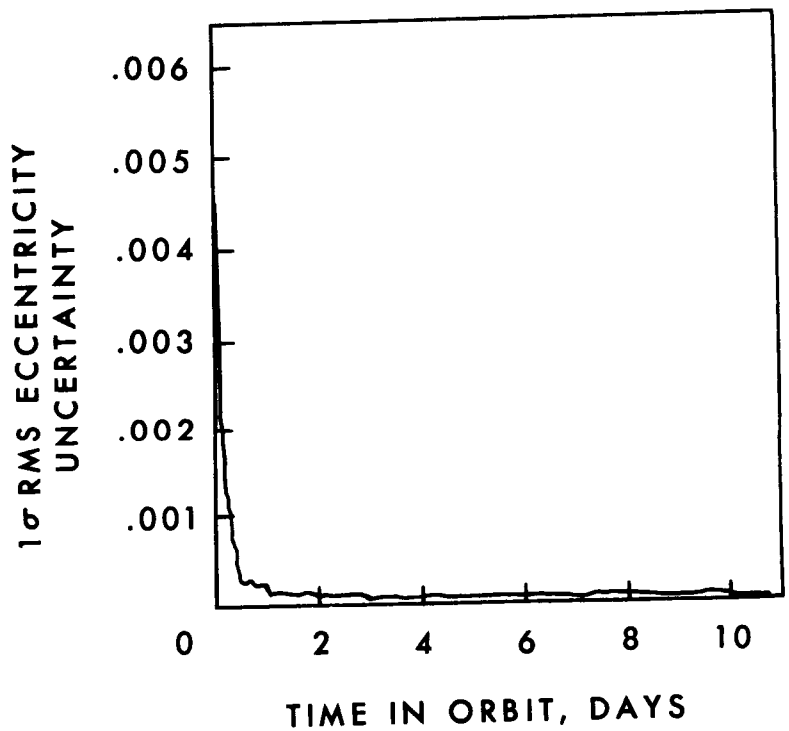

(B) RMS UNCERTAINTY FOR ECCENTRICITY.

FIGURE 4.- RMS UNCERTAINTY FOR ORBITAL ELEMENTS USING THE COMBINATION OF STAR-HORIZON AND UNKNOWN LANDMARK MEASUREMENTS.

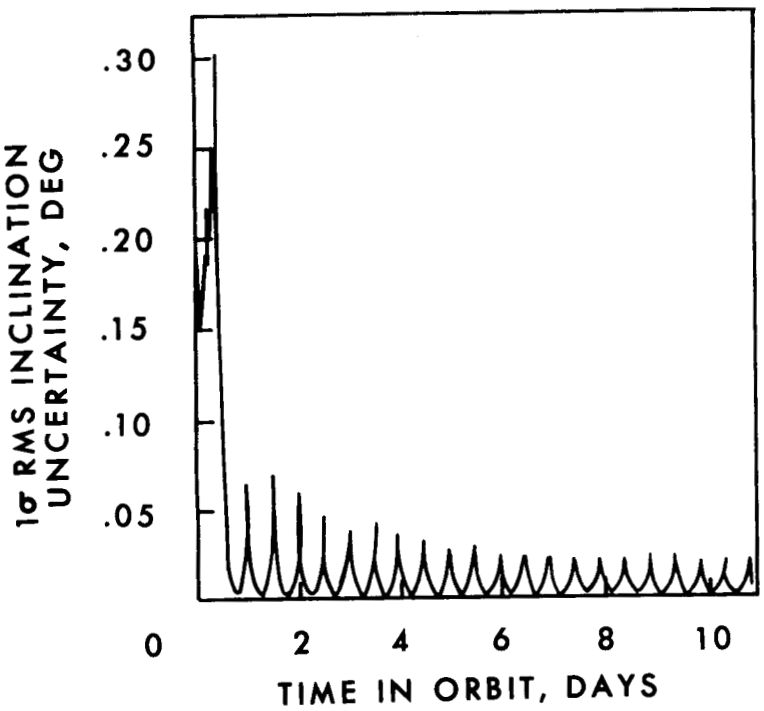

(C) RMS UNCERTAINTY FOR INCLINATION.

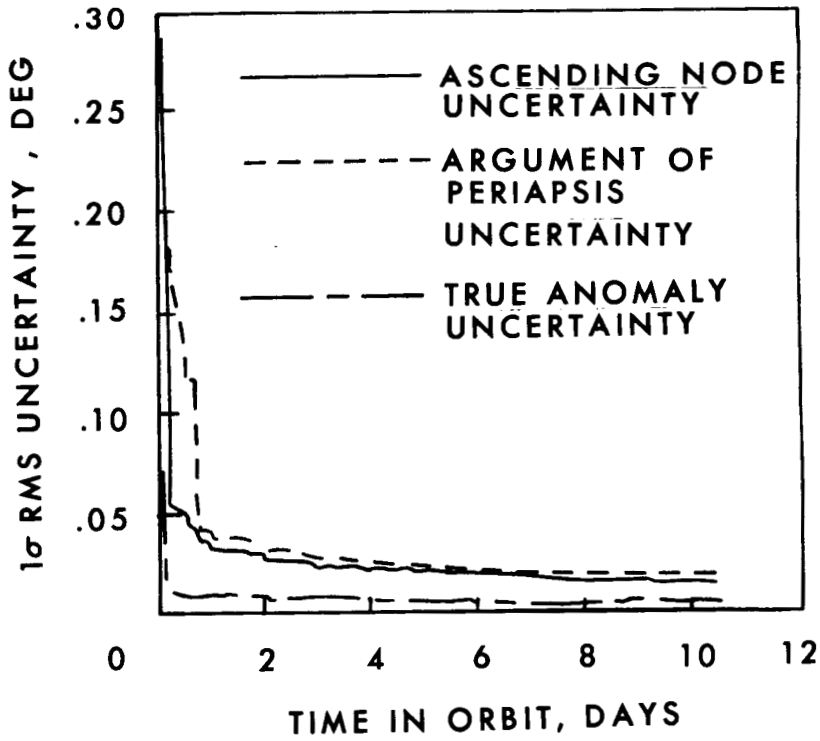

(D) RMS UNCERTAINTY FOR ARGUMENT OF PERIAPSIS, ASCENDING NODE, AND TRUE ANOMALY.

FIGURE 4.- CONCLUDED.

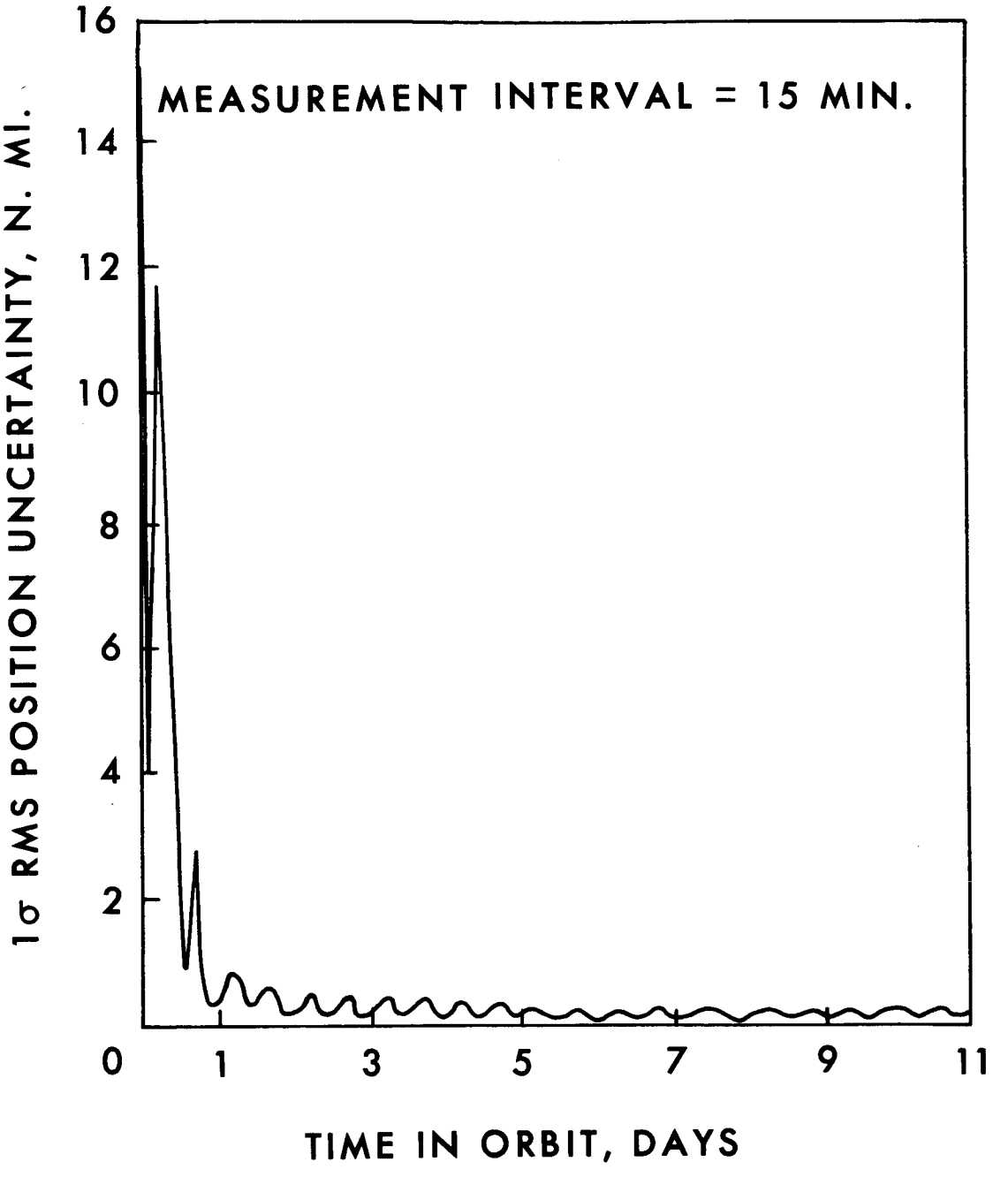

FIGURE 5.- RMS POSITION ACCURACY FOR SURFACE BEACON TRACKING ASSUMING NO BEACON LOCATION ERRORS (RANGE-RATE TRACKING ONLY).

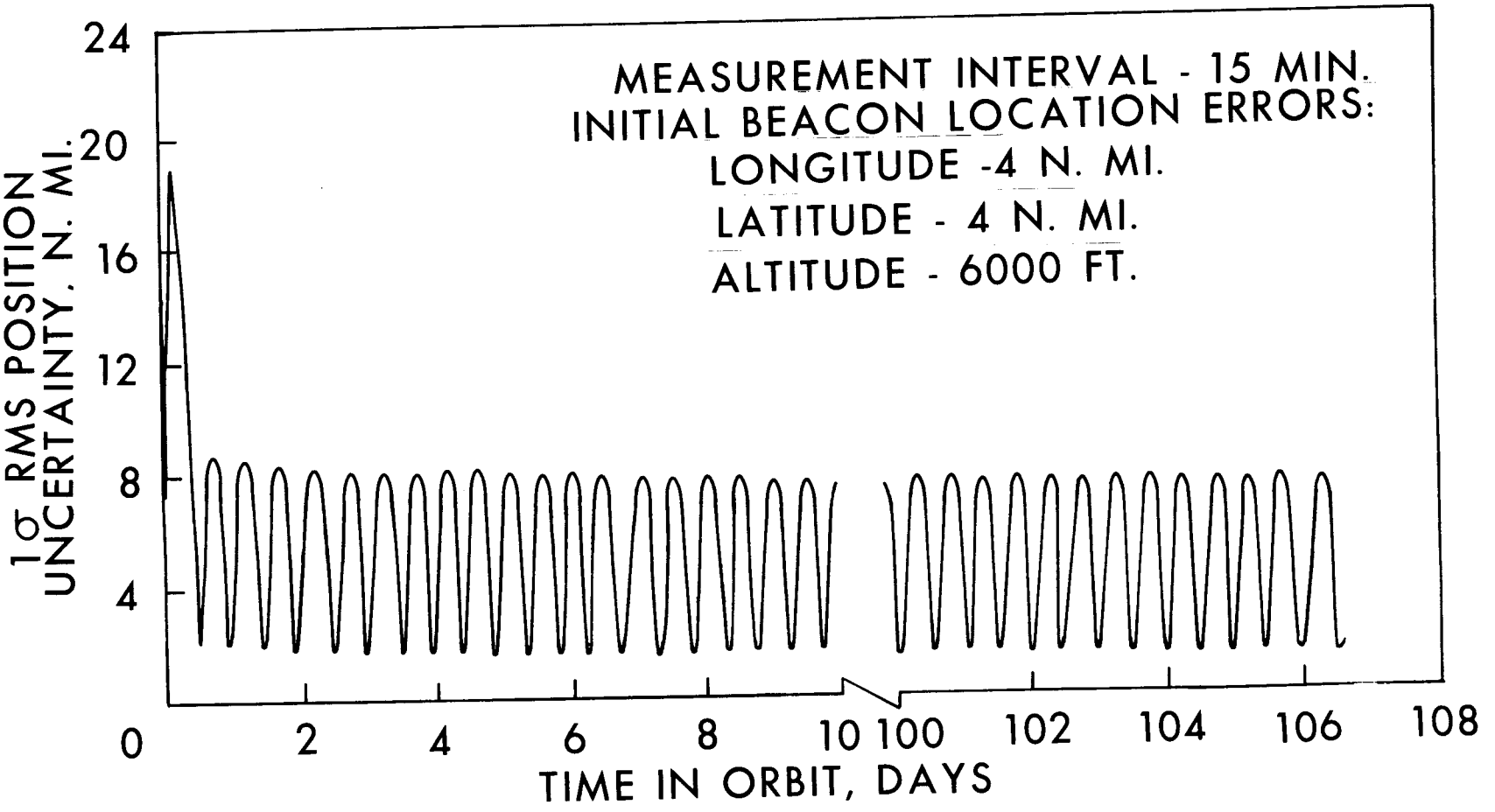

FIGURE 6.- RMS POSITION ACCURACY FOR RANGE-RATE TRACKING USING 10 SURFACE BEACONS (LOCATION ERRORS ESTIMATED).

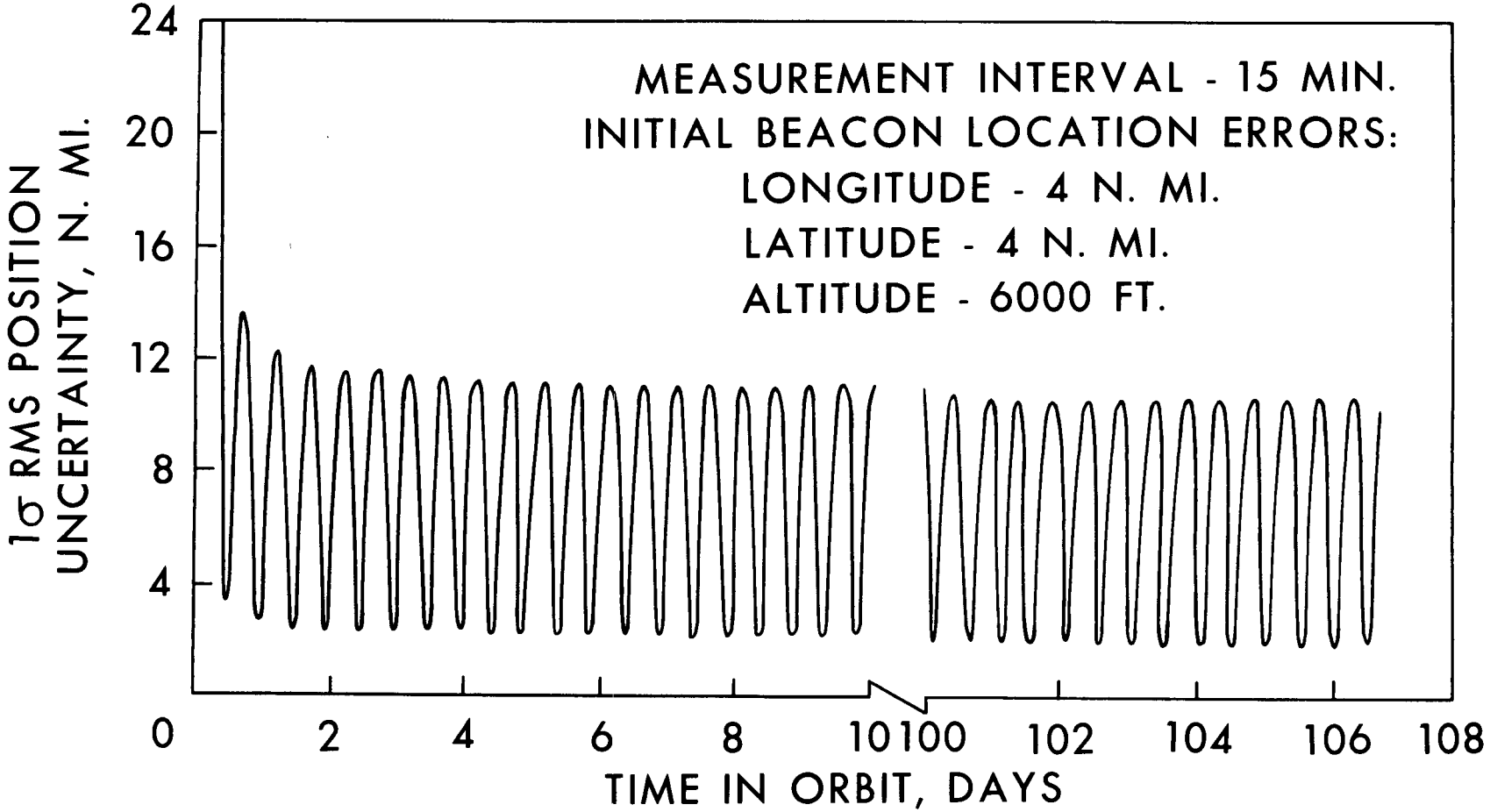

FIGURE 7.- RMS POSITION ACCURACY FOR RANGE-RATE TRACKING USING 4 SURFACE BEACONS (LOCATION ERRORS ESTIMATED).

REFERENCES

1. Bond, Victor R.: Matched-conic Solutions to Round-trip Interplanetary Trajectory Problems that Insure State-vector Continuity at all Boundaries. NASA TND-4942, 1969.

2. Lowes, F. B.; and Murtagh, T. B.: Navigation and Guidance Systems Performance for Three Typical Manned Interplanetary Missions. NASA TND-4629, 1968.

3. Taylor, J. J.; and Wilson, S.: A Minimum Energy Mission Plan for the Manned Exploration of Mars. NASA TN to be published, preprint no. S-209.

4. Thibodeau, J. R.; and Zambo, G. A.: Parking Orbits Alined Using Planetary Oblateness for Direct Mars Missions Between 1975 and 1988. MSC IN 68-FM-310, December 30, 1968.

5. Levine, G. M.: A Method of Orbital Navigation Using Optical Sightings to Unknown Landmarks. AIAA Journal, Volume 4, pp. 1928 - 1931, 1966.

6. Marcher, William: A Unified Method of Generating Conic Solutions. MIT Report R-479, 1965.

7. Murtagh, T. B.; Lowes, F. B; and Bond, V. R.: Navigation and Guidance Analysis of a Mars Probe Launched from a Manned Flyby Spacecraft. NASA TND-4512, 1968.

8. Battin, R. H.: Astronautical Guidance. McGraw-Hill Book Company, Inc., 1964.

9. Anom: User's Manual for Mark II Error Progagation Program. Philco WDL-TR 2758, February 15, 1966.

10. Murtagh, T. B.: Planetary Probe Guidance Accuracy Influence Factors for Conjunctive Class Missions. NASA TND-4852, 1969.